

---

# Basics of Lasers

## DYNAMICS OF LASER - PULSED REGIMES

---

### 4.1 Introduction

There are typically two operational regime for a laser:

- CW: continuous wave regime
- pulsed

Pulse are usually the results of a modulation of one parameter, or because of the presence of a nonlinearity placed inside the cavity. Depending on the time scale of this modulation, the pulse will have different time scale:

- Evolution at the time scale of the inversion of the population: *ns*-scale pulse laser.
- Evolution at the time scale of the phases: *ps*-*fs* pulse laser.

In the present chapter, we will look at different processes to generated pulse:

1. *Q*-switch
2. Mode-locking

### 4.2 Dynamics of laser - several classes

#### 4.2.1 rate equations

We have seen in a previous chapter that we could model the active medium of a laser with a set of two equations:

$$\dot{I} = kI(D - 1) \tag{4.1a}$$

$$\dot{D} = \gamma_{\parallel} [A - (1 + I)D] \tag{4.1b}$$

In these equation,  $I$  is the dimensionless intensity,  $D$  the inversion of population with respect to the inversion of population at threshold, and  $A$  is the pumping

Table 4.1: Laser characteristics

| Laser type  | $\gamma_{\parallel}$ [ $s^{-1}$ ] | $k$ [ $s^{-1}$ ]   | $\gamma = \gamma_{\parallel}/k$ |
|---|-----------------------------------|--------------------|---------------------------------|
| CO <sub>2</sub> <sup>†</sup>                      | $3 \times 10^4$                   | $9.6 \times 10^6$  | $3.125 \times 10^{-3}$          |
| Solid-state (Nd <sup>3+</sup> :YAG <sup>†</sup> ) | $4.166 \times 10^3$               | $6.6 \times 10^7$  | $6.31 \times 10^{-4}$           |
| Semi-cond. (AsGa <sup>‡</sup> )                   | $2.5 \times 10^8$                 | $9 \times 10^{11}$ | $2.8 \times 10^{-4}$            |
| He-Ne <sup>‡</sup>                                | $6.6 \times 10^6$                 | $3.1 \times 10^6$  | 2.15                            |

<sup>†</sup> Data from ref. [1]

<sup>‡</sup> Data from ref. [2]

rate. The only dimension remaining is the time since  $1/k$  is the lifetime of the photon in the cavity, referring to the loss of the cavity and  $1/\gamma_{\parallel}$  is the lifetime of the upperlevel contributing to the lasing process.

As we can see from table 4.2.1, it is interesting to introduce the dimensionless parameter  $\gamma = \gamma_{\parallel}/k$ . Studying the dynamics for various range of  $\gamma$  then leads to a general understanding of many different type of lasers. The system (4.1) then becomes

$$I' = I(D - 1) \quad (4.2a)$$

$$D' = \gamma[A - D(1 + I)] \quad (4.2b)$$

These equations have two sets of solutions depending whether the laser is on or off

$$(a) \text{ Laser off } \begin{cases} I = 0 \\ D = A \end{cases} \quad (b) \text{ Laser on } \begin{cases} I = A - 1 \\ D = 1 \end{cases} \quad (4.3)$$

Previously we used a physical argument (the intensity cannot be negative) to figure out which of these solutions corresponds to the laser on. At this stage though it is important to go beyond this simple approach and to perform a linear stability analysis of this system of equation.

## 4.2.2 Linear stability analysis

Stability of the steady states can be analyzed by introducing small deviation to the stationary solution ( $I^*, D^*$ ) as

$$\delta I = I^* - I \quad (4.4a)$$

$$\delta D = D^* - D \quad (4.4b)$$

Inserting these in the set of eq. (4.2) and keeping only first order terms lead to

$$\frac{d}{d\tau} \begin{pmatrix} \delta I \\ \delta D \end{pmatrix} = \mathcal{J} \begin{pmatrix} \delta I \\ \delta D \end{pmatrix} \quad (4.5)$$

where  $\mathcal{J}$  is the Jacobian of the system of equations (4.2):

$$\mathcal{J} = \begin{bmatrix} D^* - 1 & I^* \\ -\gamma D^* & -\gamma(1 + I^*) \end{bmatrix} \quad (4.6)$$

The general solution of eq. (4.5) is a linear combination of two exponential solutions:  $\delta I = c_1 \exp(\lambda_1 \tau)$  and  $\delta D = c_2 \exp(\lambda_2 \tau)$ , where  $\lambda_{1,2}$  are the eigenvalues of the Jacobian. A solution is stable, if a small deviation from the solution does not diverge. This can only be the case if  $Re(\lambda_{1,2}) < 0$ . Then small perturbation will decay to zero, and the system will relax to the steady state.

The eigenvalues can be found by solving the *characteristic equation*:

$$\begin{aligned} \lambda^2 - \text{tr}(\mathcal{J}) + \det(\mathcal{J}) = \\ \lambda^2 - \lambda [D^* - 1 - \gamma(1 + I^*)] + \gamma(1 + I^* - D^*) = 0 \end{aligned}$$

### **Solution below threshold : laser off**

For the non-lasing solution, the Jacobian writes simply as:

$$\mathcal{J} = \begin{bmatrix} A - 1 & 0 \\ -\gamma A & -\gamma \end{bmatrix} \quad (4.8)$$

for which the eigenvalues are solutions of

$$\det(\mathcal{J} - \lambda \mathbf{1}) = (A - 1 - \lambda)(-\gamma - \lambda) = 0 \quad (4.9)$$

This readily leads to the eigenvalues:

$$\lambda_1 = A - 1 \quad \text{and} \quad \lambda_2 = -\gamma \quad (4.10)$$

which are simultaneously negative only when  $A < 1$ . This solution is therefore stable below the threshold, and unstable above it.

### **Solution above threshold : laser on**

For the lasing solution ( $I^* = A - 1, D^* = 1$ ) the characteristic equation is

$$\lambda^2 + \gamma A \lambda + \gamma(A - 1) = 0 \quad (4.11)$$

To analyze the stability, we can notice that<sup>1</sup>

$$\lambda_1 \lambda_2 = \frac{c}{a} = \gamma(A - 1) \quad (4.12a)$$

$$\lambda_1 + \lambda_2 = -\frac{b}{a} = -\gamma A \quad (4.12b)$$

From eq. (4.12a), we can say that both root have the same sign if and only if  $A > 1$ . Moreover, since the sum is negative, for  $A > 1$  both roots are negative: the solution is stable. Although we find the same results are previously this analysis allows to go beyond the simple stability criterion and describes the relaxation behaviour of the laser.

Since the stability of the system depends on the real part of the eigenvalue solution of Eq. (4.2), we can fully look at the eigenvalues of the system. The discriminant being

$$\Delta = (\gamma A)^2 - 4\gamma(A - 1) \quad (4.13)$$

For large value of  $\gamma$ ,  $\Delta > 0$  and eigenvalues are

$$\lambda_{\pm} = -\frac{\gamma A}{2} \pm \frac{1}{2} \sqrt{(\gamma A)^2 - 4\gamma(A - 1)} < 0 \quad (4.14)$$

By contrast, when  $\gamma \ll 1$ , we have

$$(\gamma A)^2 \ll 4\gamma(A - 1),$$

which leads to the eigenvalues:

$$\lambda_{\pm} = -\frac{\gamma A}{2} \pm i\sqrt{\gamma(A - 1)} \quad (4.15)$$

This case is very different from the previous one. In this case, this study of linear stability of the laser solution ( $I^* = A - 1, D^* = 1$ ) shows that when the laser starts, it relaxes towards the stationary solution with a decay  $\gamma A/2$  and exhibits an oscillatory behaviour. Frequency of the oscillation is<sup>2</sup>

$$\Omega = \sqrt{k\gamma_{\parallel}(A - 1)} \quad (4.16)$$

The system (4.2), can easily be integrated (Fig. 4.1). Fig. 4.1 presents the solution of the system (4.2) for various values of  $\gamma$ . Depending of the range of  $\gamma$ , the laser may exhibit an oscillating behaviour. When oscillations are present, we call this laser: **class-B** laser, whereas it is classified as **class-A** laser in the other case.

<sup>1</sup>We remind that the solution  $x_{1,2}$  of a second quadratic equation  $ax^2 + bx + c = 0$  are such that  $S = x_1 + x_2 = -b/a$  and  $P = x_1 \times x_2 = c/a$ .

<sup>2</sup>To write the system (4.2), we have scale with respect to the lifetime of the photon in the cavity such that  $\tau = kt$ . Therefore, we have the frequency  $\Omega [s^{-1}] = \Omega' k = k\sqrt{\gamma(A - 1)}$

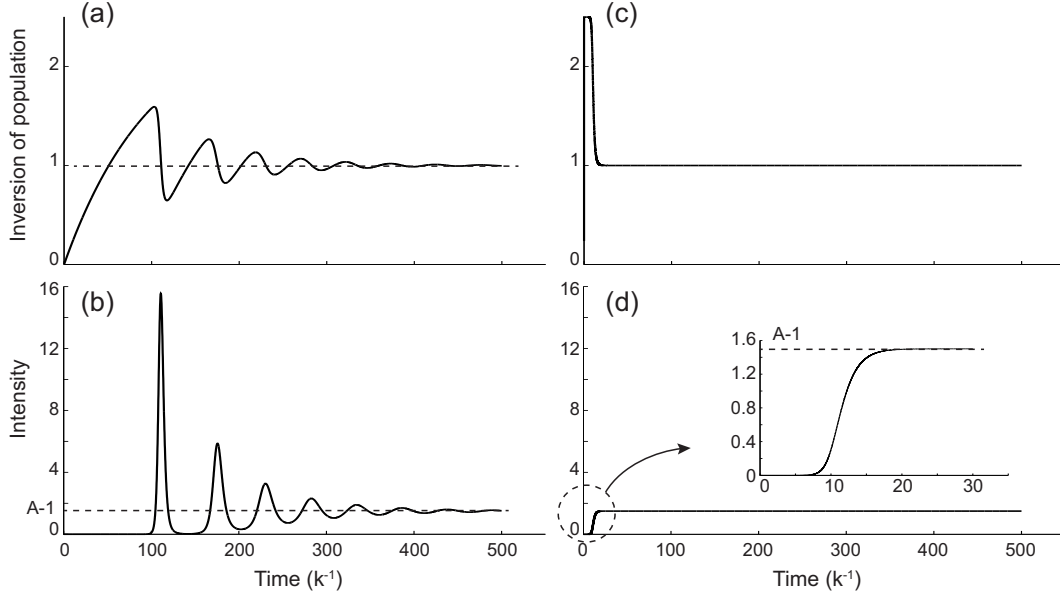


Figure 4.1: Integration of Eq. (4.2) with  $A = 2.5$ ,  $D_{\text{init}} = 0$ ,  $I_{\text{init}} = 10^{-10}$  and (a, b)  $\gamma = 0.01$  and (c, d)  $\gamma = 100$ .

### 4.2.3 class-A laser

Note that in the extrem case where  $\gamma_{\parallel} \gg k$ , the atomic variable  $D$  will relax extremely fast toward its equilibrium value. Especially, we can then consider that  $D \sim D_{\text{eq}}$  and then  $\dot{D} = 0$ . The system (4.2) becomes

$$\dot{I} = kI \left[ \frac{A}{1+I} - 1 \right] \quad (4.17)$$

For  $I \ll 1$  we can expand  $1/(1+I) \sim 1 - I$ , therefore eq. (4.17) writes as

$$\dot{I} = kI(A - 1 - AI) \quad (4.18)$$

which exhibits a quadratic behaviour. We may also look at the initial starting of the laser ( $I \sim 0$ ): the intensity grows as

$$I(t) = I_0 e^{k(A-1)t} \quad (4.19)$$

The integration of eq. (4.17) leads to a behaviour similar to the one observed previously (Fig. 4.1.d).

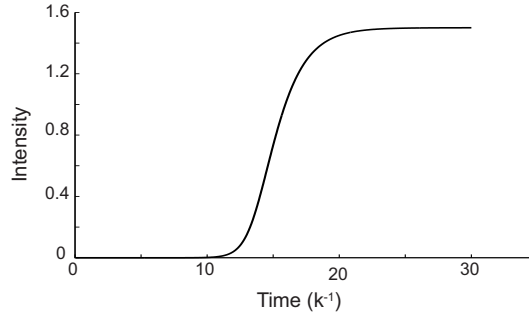


Figure 4.2: Class-A laser. Integration of Eq. (4.17) with  $A = 2.5$ ,  $k = 1$ .

## 4.3 Class-B laser and Q-switch

### 4.3.1 general case

The main observation from the starting of a class-B laser, is that it presents intense *spikes*<sup>3</sup> We can identify two important points from this figure:

1. The maximum of the peak corresponds to  $A = 1$ .
2. When the peak starts, the inversion of population  $D > 1$ .

To generate high-peak intensity, one way would be to prevent the laser to start until the inversion of population is much larger than  $D = 1$ . Numerically, this is obviously very easy to achieve, as we only need to fix the initial condition for  $D = D_0 > 1$ . Fig. 4.4 shows the starting of a class-B laser with  $D_0 = 5$ . Note that the vertical scale is very different from the one used for Fig. 4.3. The peak intensity is now  $I > 220$  when it was only  $I \sim 16$  when with start from  $D \sim 0$  for initial condition.

Experimentally, the process consists in rapidly changing the loss of the cavity, such that the lasing threshold is suddenly modified. Since loss are related to the quality factor of the cavity  $Q$ , this mechanism is called Q-switch. It consists in two steps (Fig. 4.5):

step 1: The losses of the cavity are maintained at a high value ( $k_+$ ). The inversion of population grows. The lasing threshold is  $D_{\text{th}}^+ = \frac{k_+}{\sigma c}$

step 2: When  $D \sim D_{\text{th}}$ , the losses are switched to a low value ( $k_-$ ). The threshold of the laser is in this case:  $D_{\text{th}}^- = \frac{k_-}{\sigma c} \ll D_{\text{th}}^+$ . The corresponding pumping

<sup>3</sup>For the first observation, and the derivation of the equation, see Tang Statz and deMars paper.

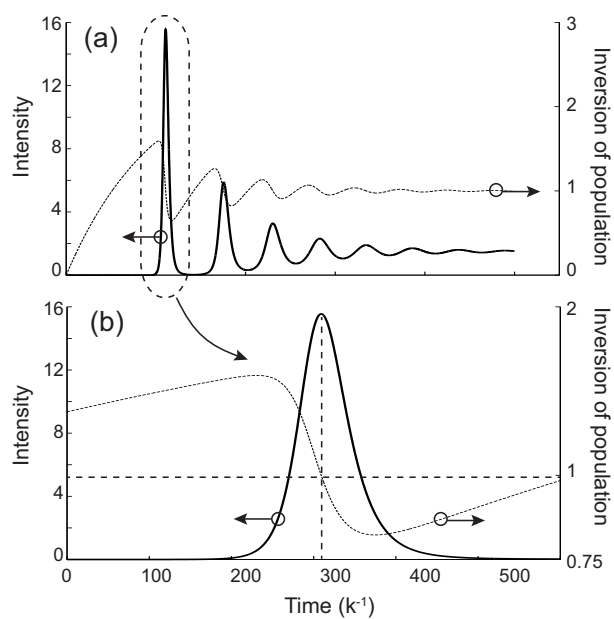


Figure 4.3: Spiking of a class-B laser at starting. Integration of Eq. (4.2) with  $A = 2.5$ ,  $\gamma = 0.01$ ,  $I_{\text{init}} = 10^{-10}$  and  $D_{\text{init}} = 0$

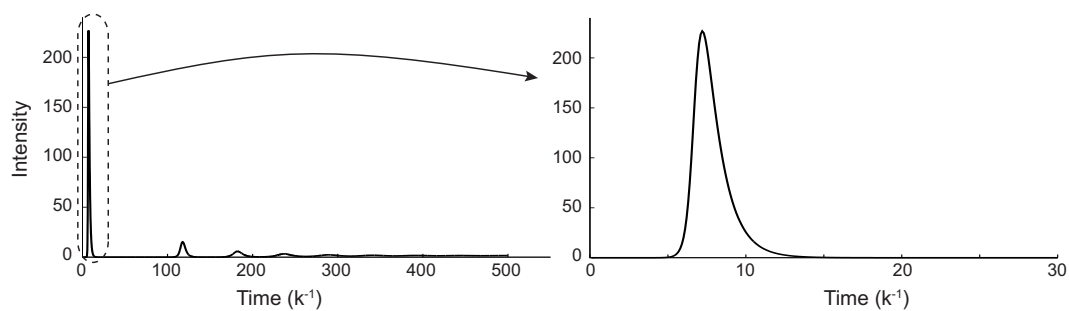


Figure 4.4: Integration of Eq. (4.2) with  $A = 2.5$ ,  $\gamma = 0.01$ ,  $I_{\text{init}} = 10^{-10}$  and  $D_{\text{init}} = 5$

rate is then  $A = \frac{D}{D_{\text{th}}} \gg 1$ . The excited level is rapidly depleted, and a giant pulse is emitted.

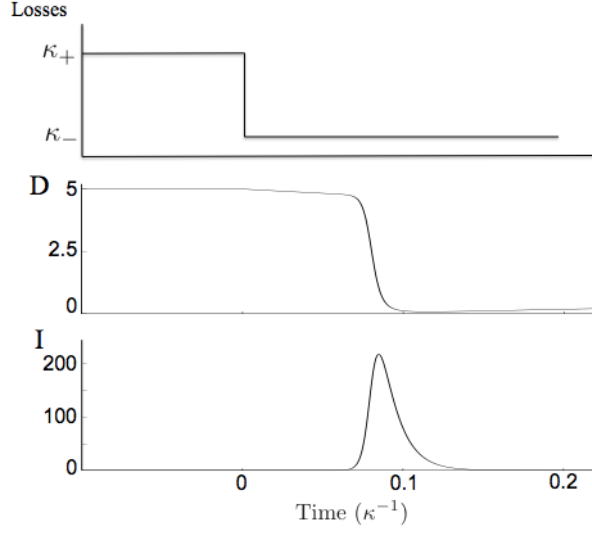


Figure 4.5: Mecanism of  $Q$ -switching operation.

### 4.3.2 model for the peak intensity

During the emission of the pulse, we can consider that only the stimulated emission needs to be taken into account. Rate equations for the laser are then:

$$\dot{I} = kI(D - 1) \quad (4.20a)$$

$$\dot{D} = -\gamma_{\parallel}DI \quad (4.20b)$$

Since we are looking at the intensity, we can then write

$$\frac{dI}{dD} = \frac{kI(D - 1)}{-\gamma_{\parallel}DI} = \frac{\kappa}{D} - \kappa \quad (4.21)$$

with  $\kappa = k_-/\gamma_{\parallel}$ . We can integrate Eq. (4.21):

$$I(t) = I(t_0) - \kappa [D(t) - D(t_0)] + \kappa \ln \frac{D(t)}{D(t_0)} \quad (4.22)$$

which becomes

$$I = \kappa \left( \ln \frac{D}{A} + A - D \right) \quad (4.23)$$

because, at  $(t = 0)$ , we have  $I = 0, D = A$ . Eq. (4.23) is drawn on Fig. 4.6 with  $\kappa = 100$  for different values of  $A$ . In the case where the initial inversion of population  $D = A$  is very large compare to the inversion at threshold  $D = 1$ , then the peak intensity can be simply expressed by:

$$I_{\text{peak}} = \kappa(A - \ln A - 1) \quad (4.24)$$



Obviously, the larger  $A$ , the larger the peak intensity. But also, the smaller the decay rate of the photon  $k_-$  compare to the relaxation of the level  $\gamma_{||}$ , the larger is  $\kappa$  and then the peak intensity. For peak of a few nanosecond, gigawatts peaks are possible to achieve.

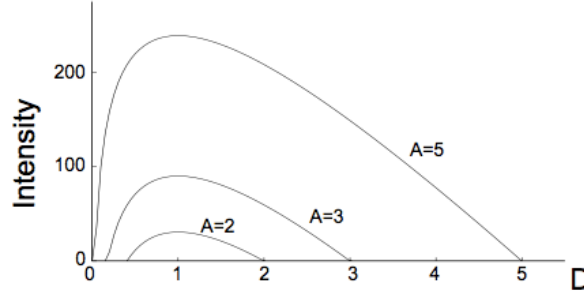


Figure 4.6: Evolution of the intensity *vs* the inversion of population  $D$  for a  $Q$ -switch pulse, for different values of the pumping rate  $A$ .

### 4.3.3 passive $Q$ -switch

There are many ways to achieve pulses by  $Q$ -switching. Here we discuss a very common way: the inserion of a saturable absorber inside the laser cavity. As we will see later, such device may also be used to achieve *mode-locked* pulse for which the mechanism is totally different. It is however important to see that the inserion of nonlinear loss may lead to a periodic stable solution: the  $Q$ -switched pulses. For simplicity, the nonlinear loss of a fast saturable absorber (relaxation time much shorter than pulse duration) can be modeled as

$$k(I) = \frac{k_0}{1 + \alpha I} \quad (4.25)$$

where  $k_0$  are the linear inserion loss, and  $\alpha$  the saturability of the absorber<sup>4</sup>. This has the property to exhibit nonlinear loss  $k(I)$  (Fig. 4.7):

We may start our analysis from the traditional set of equations for the class-B laser, for which we add the nonlinear loss  $k(I)$  as follow:

$$\dot{I} = I(D - 1) - k(I)I \quad (4.26a)$$

$$\dot{D} = \gamma[A - (1 + I)D] \quad (4.26b)$$

<sup>4</sup>There exists different type of saturable absorber. This can be a crystal [...] or it can be combined with one of the mirror of the cavity.

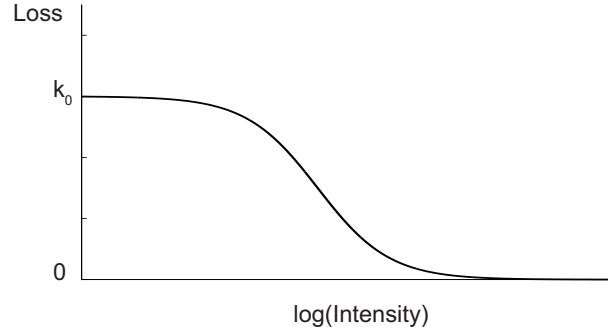


Figure 4.7: typical response from a saturable absorber or a saturable mirror: the insertion losses decrease as the incident intensity increases.

As we did previously, may look at the stability of the lasing solution ( $I_s \neq 0, D_s = 1$ ). We will also suppose that we can write the class-B model such that  $k(I_s) = 0$ . The Jacobian of the Eq. (4.26) is

$$J = \begin{bmatrix} (D-1) - \left(\frac{\partial k}{\partial I}\right) I - k(I) & I \\ -\gamma D & -\gamma(1+I) \end{bmatrix} \xrightarrow[k(I_s)=0]{\begin{pmatrix} I_s \\ D_s \end{pmatrix}} \begin{bmatrix} -\left(\frac{\partial k}{\partial I}\right) I_s & I_s \\ -\gamma & -\gamma(1+I_s) \end{bmatrix}$$

Using a multiscale approach (see appendix), we can calculate the eigenvalue of the Jacobian:

$$\lambda_{\pm} = -\frac{\gamma A}{2} - \left(\frac{\partial k}{\partial I}\right) \pm \sqrt{\gamma(A-1)} \quad (4.27)$$

Since  $\left(\frac{\partial k}{\partial I}\right) < 0$ , we clearly see that the introduction of the nonlinear losses in the system may lead positive real part of the eigenvalue: the solution ( $I_s, D_s = 1$ ) becomes unstable, and for this parameter, the system enters a periodic regime: the Q-switch regime.

As previously done without the presence of nonlinear loss (see bifurcation diagram for the class-B laser), we can draw the bifurcation diagram when the saturable absorber is introduced (Fig. 4.8).

## 4.4 Mode-locking

There exist another way to generate pulses. As we mentioned above, to generate pulses, we need to impose a modulation on the system. This can be the pumping rate, the losses... etc. For a modulation at the time scale of the evolution of

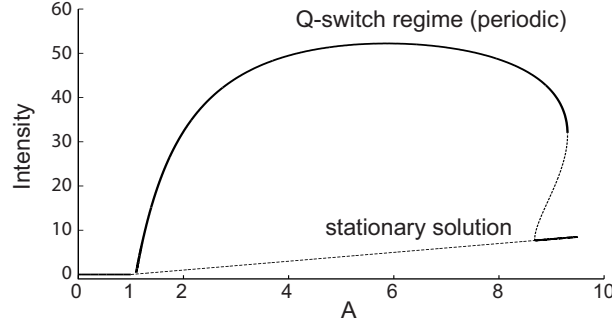


Figure 4.8: bifurcation diagram representing the solution of the system (4.26). The solid line are stable state whereas dashed line are for unstable states. The solution corresponding to the laser Off is not shown.

phases, the process is called *mode-locking* for a reason that will become clearer in the next pages.

#### 4.4.1 longitudinal modes

We have already see (cf. chapter on cavity) that for a Fabry-Perot cavity, terminated by two mirrors  $R_1 = R_2 = R$  the transfert function was periodic, with a period equal to the free-spectral range:

$$\Delta\nu_F = \frac{c}{2\ell} \quad (4.28)$$

where  $\ell$  is the distance between the two mirrors (Fig. 4.9). The transferred intensity ( $I_T$ ) for such Fabry-Perot is given by:

$$I_T = \frac{I_0}{1 + \frac{4R}{T^2} \sin^2 \frac{\phi}{2}} = \frac{I_0}{1 + \frac{4R}{T^2} \sin^2 \left( \frac{\pi\nu}{\Delta\nu_F} \right)} \quad (4.29)$$

#### 4.4.2 mode-locking

Such response function presents multiple resonances. And for each resonance, there exists one oscillating mode, which may participate to the resulting output field. Obviously the total number of modes that will eventually oscillated simultaneously inside the cavity also depends on the properties of the gain medium. For the moment, we will suppose that the gain has a “bell-shape” (Fig. 4.10).

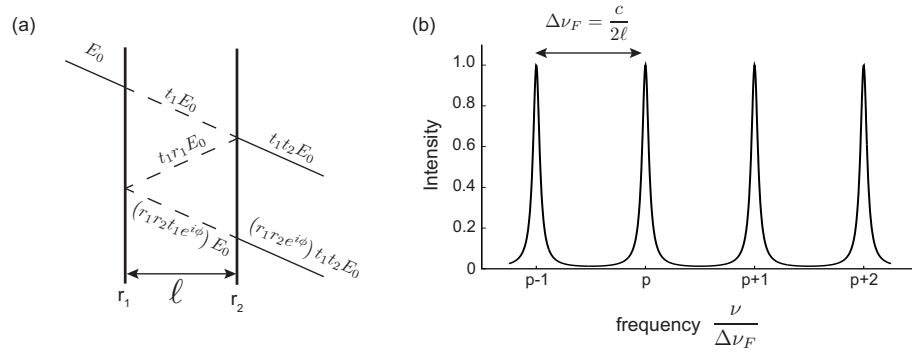


Figure 4.9: (a) Fabry-Perot cavity. Its length is  $\ell$ ,  $r_1$  and  $r_2$  are the reflection coefficient of the mirrors. (b) the associated transfer function for  $R = r_1^2 = r_2^2 = 0.95$  the reflection coefficient in intensity.

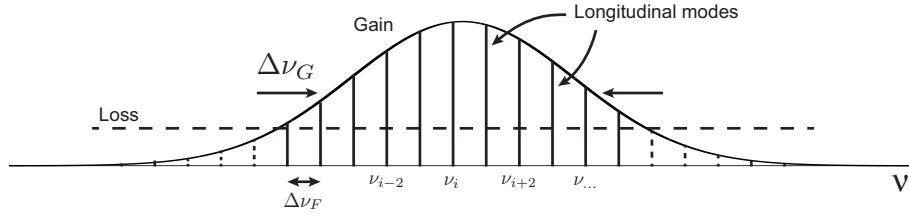


Figure 4.10: longitudinal modes amplified by the gain medium.  $\Delta\nu_G$  is the FWHM of the gain, and  $\Delta\nu_F$  the free spectral range. Vertical dashed line are the longitudinal modes, which cannot participate to the lasing process because of loss.

The output field results from a superposition of the  $N$  oscillating modes inside the cavity:

$$E(t) = \sum_{p=0}^N A_p e^{i\phi_p} e^{i\omega_p t} \quad (4.30)$$

$A_p$  is the amplitude of the mode  $p$  and  $\phi_p$  its phase. Depending on the relative phase of each mode  $\phi_p$  this sum can result in drastically different manner.

### random phases

As we can see on Fig. 4.11, when the phases of the different modes of the cavity are randomly chosen, and are not fixed from each other, the resulting field presents a noisy behaviour. The average power coming out of the laser is simply the sum of each power  $P_p$ :

$$\langle P \rangle = \sum \langle P_p \rangle \quad (4.31)$$

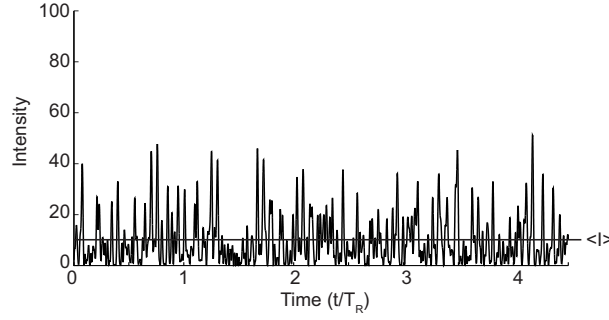
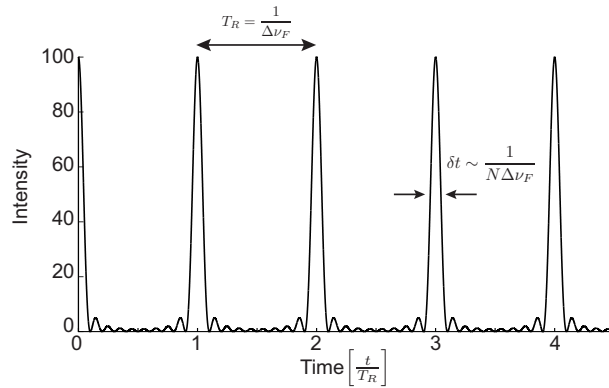


Figure 4.11: superposition of 10 modes with random phases

### locked phases

The situation is drastically different when we fix the relationship between the phase  $\phi_p$  of each modes. Suppose now that  $\{\forall p \mid A_p = A_0; \phi_p = 0\}$ . Then we can rewrite this equation (4.32) by writing  $\omega_p = \omega_0 \pm p\Delta\nu_F$  and do the sum:

$$E(t) = A_0 e^{i\omega_0 t} \sum_{p=-\frac{N-1}{2}}^{\frac{N-1}{2}} = A_0 \frac{\sin\left(\frac{N\Delta\nu_F t}{2}\right)}{\sin\left(\frac{\Delta\nu_F t}{2}\right)} \quad (4.32)$$

Figure 4.12: constructive interference of  $N = 10$  longitudinal modes simultaneously oscillating inside a laser cavity.  $T_R$  is the return time inside the cavity.

The task of mode-locking is to obtain a coherence superposition of the larger number of modes (synchronous oscillation) such that the superposition of these modes forms a pulse that spatially extends over a length much shorter than the cavity length.

As an example, we may take the typical parameter for a commercial Ti:Sa laser is 3 m. For a 100 fs long pulse, the pulse is actually  $cdt \sim 3$  mm long. The ratio in length is then 1/1000. We can then picture the pulse as a 3 mm-long pancake of light travelling inside the cavity, and releasing some energy at each round-trip as it reflects on the output coupler, the terminal mirror ( $R < 1$ ). Each pulse that come out of the laser cavity is actually one single pulse travelling around the cavity. This is very different from  $Q$ -switch pulses for which the energy has to grow (increase of the inversion of population) before it is suddenly released. The pulse duration is in this case longer than the cavity round-trip time.

### 4.4.3 passive mode-locking

As for passive  $Q$ -switching, the use of saturable absorber may lead to the generation of pulse by modulation of the loss of the cavity. As we already said, mode-locked pulses require fast modulation of these losses. This is a condition that needs to be also taken into account [3]. If  $\tau_a$  is the relaxation time of the saturable absorber, and  $\tau_G$  the recovery of the gain, then a condition to use this process is

$$\tau_a < \tau_G < T_R \quad (4.33)$$

This condition obviously imposes the choice of saturable absorber, but also the length of the laser cavity!

#### shapping of pulse

A simple way to explain the formation of mode-locked pulse is to look at the combined influence of gain and saturable loss in the time domain. Suppose that we have already a pulse inside the cavity, the action of the saturable absorber and the gain is depicted on fig. 4.13. Note that the response time of the saturable, although it must fulfill the condition (4.33), this response may be fast or slow compare to the final duration of the pulse. Theory of mode-locking using fast and slow saturable absorber have both been heavily developped since the first demonstration of passive mode-locking [4, 5].

We can clearly see from this very simplified schematics that as the pulse evolves inside the cavity, it experiences both the gain and the saturable absorber, resulting into a short pulse. We will see later that the pulse may experiences other effect such as dispersion, which then limit the efficiency of the above-mentionned process.

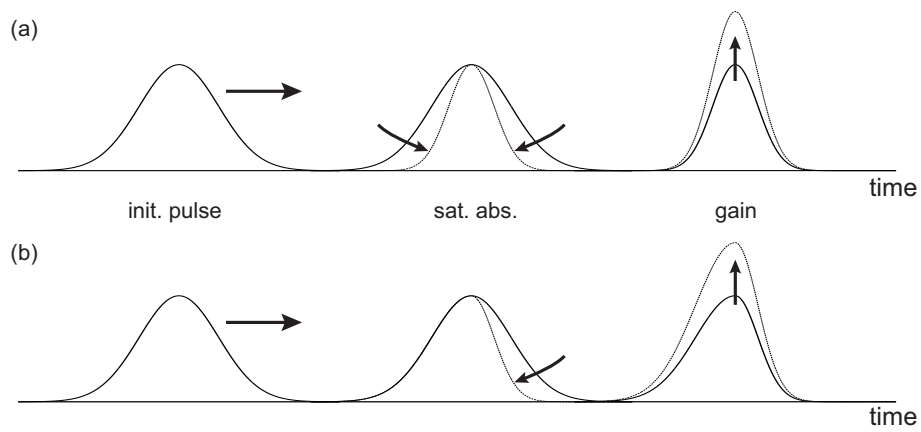


Figure 4.13: shaping of mode-locked pulse by the combined action of the gain and the fast (a) and slow (b) saturable absorber.





# Bibliography

- [1] Thomas Erneux and Pierre Glorieux. *Laser Dynamics*. Cambridge University Press, 1<sup>st</sup> edition, June 2010.
- [2] Orazio Svelto. *Principles of Lasers*. Springer, December 2009.
- [3] Claude Rullière, editor. *Femtosecond Laser Pulses: Principles and Experiments*. Springer, 1<sup>st</sup> edition, October 1998.
- [4] Anthony E. Siegman. *Lasers*. University Science Books, 1<sup>st</sup> edition, May 1986.
- [5] Herman A. Haus. Mode-locking of lasers. *IEEE J. selected topics in Quant. electr.*, 6(6):1173–1185, 2000.